doi:10.1017/S1431927622003221
Microsc. Microanal. 28 (Suppl 1), 2022


# Relation Between Composition, Structure and Properties of Different Dental Alloys

Adriana Saceleanu[1], Nestor Florido-Suarez[2], Cristina Jimenez-Marco[2], Julia Mirza-Rosca[2*]

[1.] "Lucian Blaga"University of Sibiu, Medicine Faculty, 550024 Sibiu, Romania
[2.] University of Las Palmas de Gran Canaria, Mechanical Engineering Department., University Campus of Tafira, Engineering Building, 35017 Las Palmas de Gran Canaria, Spain
* Corresponding author: julia.mirza@ulpgc.es

## INTRODUCTION

The use of dental alloys as a material for bridges, crowns and prostheses is currently being investigated, taking into account their biocompatibility, as the material must be non-toxic and not cause allergies, inflammation or other reactions affecting the body [1].
In this field, Co-Cr and Ni-Cr based alloys are often used, as they have good corrosion resistance and high wear resistance due to the crystalline nature of cobalt and nickel [2,3]. In addition, Ni-Cr and Co-Cr alloys have been used in the field of dentistry for porcelain or porcelain-fused-to-metal crowns due to their good biocompatibility, wear resistance, long service life, good mechanical properties and superior corrosion [4–6].

## PURPOSE

A study of the effects of corrosion and mechanical properties as well as a comparison of the heat treatment of Ni-Cr and Co-Cr dental alloys containing molybdenum and silicon in their composition is carried out (see the composition wt% in Table 1).

## EXPERIMENTAL

As a previous step to electrochemical, metallographic and flexural tests, several processes should be performed, such as to embed into an epoxy resin cylinder the samples for cutting and their subsequent polishing in two stages: polishing with SiC abrasive papers of progressive grain size from 400 to 2500 grit and final polishing with 0.1 µm alpha alumina suspension.

Table 1. Samples main composition (wt%)

| Sample | Ni | Co | Cr | Mo | Al | Si | W |
|---|---|---|---|---|---|---|---|
| Ni-Cr | 65.6 | - | 20.1 | 1.3 | 2.4 | 3.3 | 7.1 |
| Co-Cr | - | 59.5 | 31.5 | 5.0 | - | 2.0 | - |

The samples are then submerged in an ultrasonic machine for 5 minutes to remove all traces of dirt, and then immersed in a reagent composed of hydrochloric acid, nitric acid and glycerine for chemical etching. After electrochemical etching, the metallographic test is carried out by taking images with the metallographic microscope, enlarging 5 and 10 times the real size of a part of the Ni-Cr samples, while the Co-Cr sample is enlarged to 50 and 100 times the real image.
On the other hand, electrochemical test consists in inserting a specimen into an electrochemical cell together with Saturated Calomel Electrode (SCE) as reference and Pt electrode as counter electrode, Corrosion potential (Ecorr) was determined, and Electrochemical Impedance Spectroscopy (EIS) was applied. SEM observations were performed. Finally, three-point bending test is applied to find the value of the modulus of elasticity of each specimen.

## RESULTS

In the metallographic test, the images taken before the corrosive agent attack show some porosity and scratches on the surface of the samples. SEM observations and EDS results are presented in Fig.1 and Fig.2.

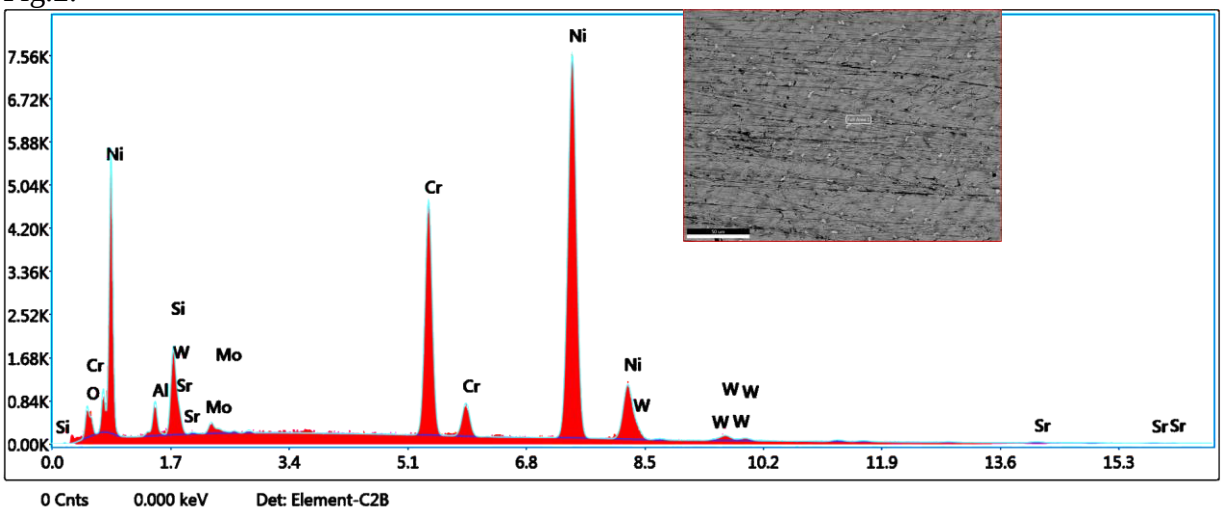


Fig.1. SEM and EDS observations of Ni-Cr sample

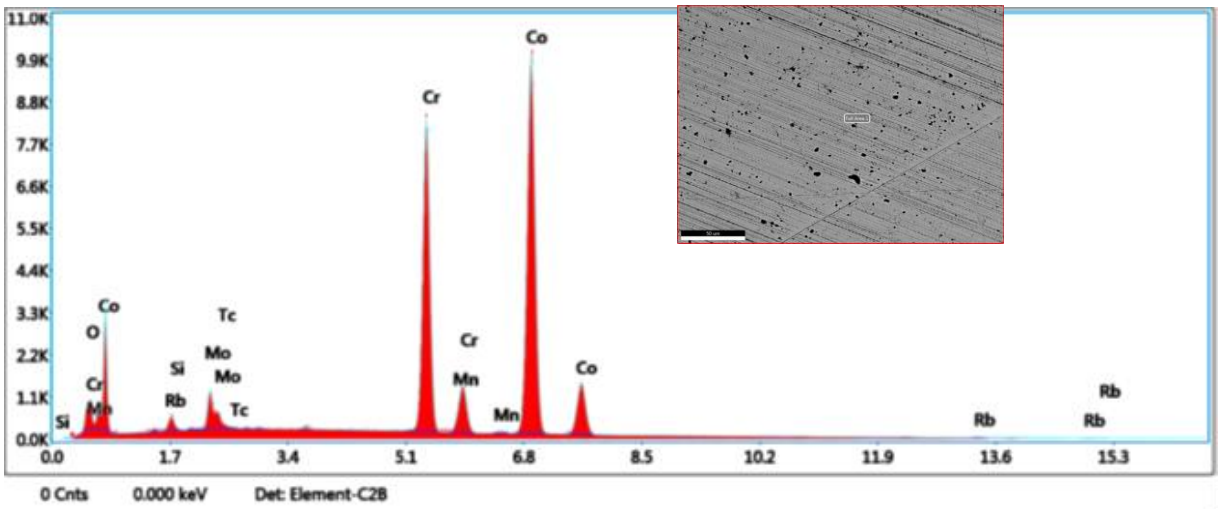


Fig.2. SEM and EDS observations of Co-Cr sample

However, both samples showed a crystalline structure after chemical etching. Moreover, in the corrosion tests, the samples are immersed in Ringer Grifols solution (see composition in Table 2) which simulates the physiological fluid of the human body the results obtained were processed by the Ec Lab program.

In the linear polarization test, potential E versus time graphics showed the tendency to passivation of each sample. In addition, the EIS method is performed on each specimen at different potentials to obtain the spectra, Nyquist plots (Fig.3 for Co-Cr alloy and Fig.4 for Ni-Cr alloy) and Bode plots (Fig.5 for Co-Cr alloy and Fig.6 for Ni-Cr alloy).

https://doi.org/10.1017/S1431927622003221 Published online by Cambridge University Press

Table 2. Composition of Ringer Grifols solution

| Compound | Composition (mmol/L) |
|---|---|
| $Cl^-$ | 111.5 |
| $Na^+$ | 130 |
| $K^+$ | 5.5 |
| $Ca^{2+}$ | 1.7 |
| $C_3H_5O_3^-$ | 27.2 |

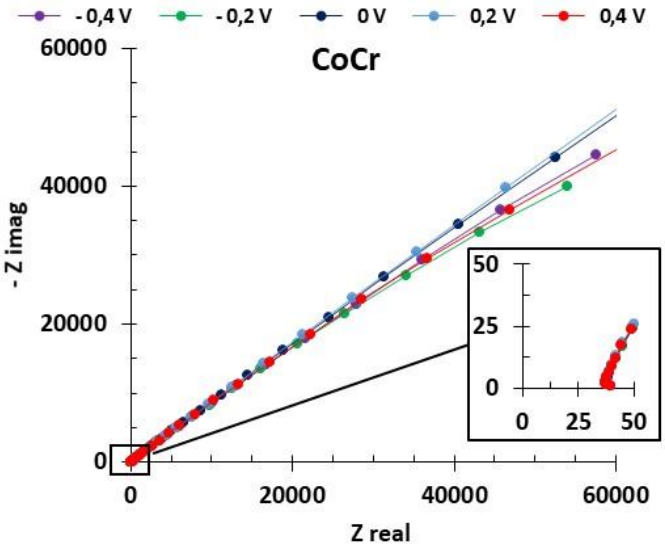


Fig.3. Nyquist plot at different potentials for Co-Cr alloy

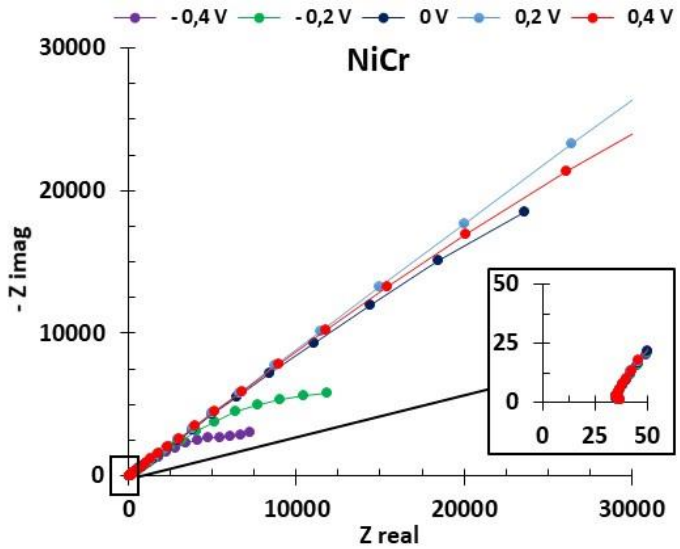


Fig.4. Nyquist plot at different potentials for Ni-Cr alloy

https://doi.org/10.1017/S1431927622003221 Published online by Cambridge University Press

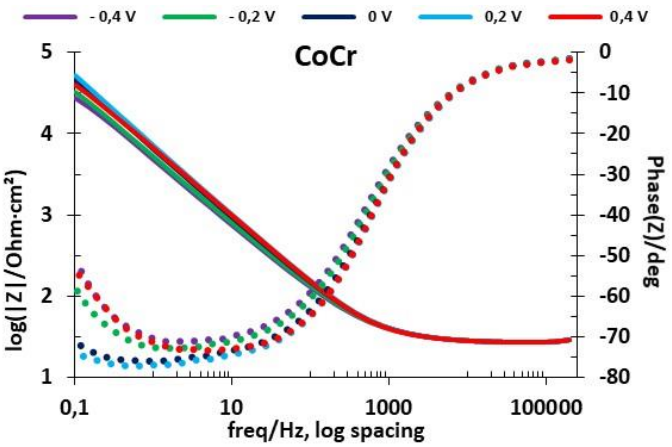


Fig.5. Bode plots at different potentials for Co-Cr alloy

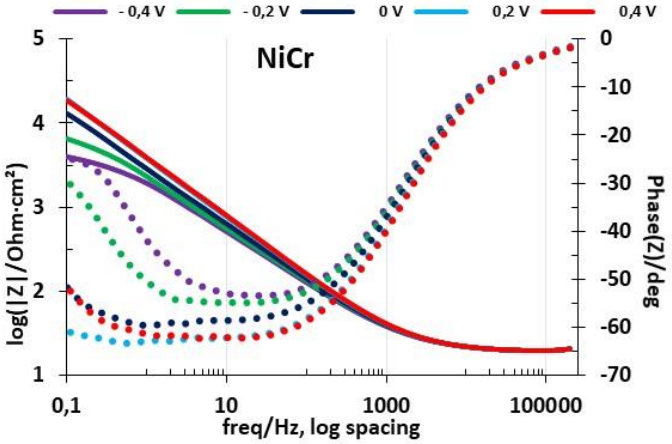


Fig.6 Bode plots at different potentials for Ni-Cr alloy

In this case, the corrosion resistance increases the more positive the applied potential and the higher the impedance and phase angle values [7]. Therefore, the Co-Cr alloy shows the highest corrosion resistance.

In the three-point bending test (Fig.7) the value obtained for the modulus of elasticity of Ni-Cr specimens is much higher than that of the Co-Cr alloy.

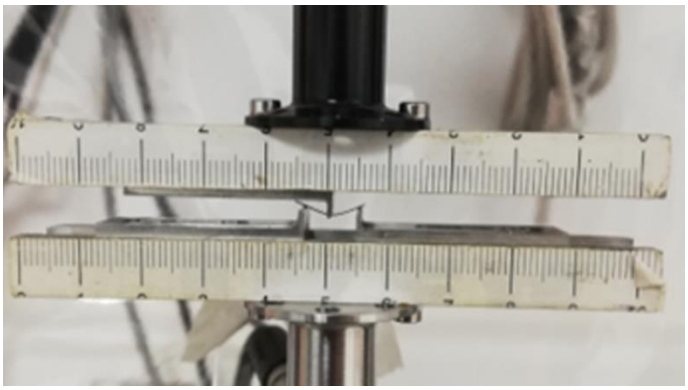

Fig.7 Three points bending test of the samples

https://doi.org/10.1017/S1431927622003221 Published online by Cambridge University Press

## CONCLUSIONS

The metallography test showed the dendritic structure of both samples, although they present some defects.

In the corrosion tests, the Co-Cr alloy has a better corrosion resistance since it shows a more positive corrosion potential, and its impedance value is upper than Ni-Cr alloy.

Besides, in the three-point bending test, Co-Cr alloy obtained a lower value of modulus of elasticity.

Nonetheless, it has not been possible to establish a clear relationship between the degree of molybdenum and silicon concentrations in the alloys and the electrochemical corrosion behaviour [8].

## REFERENCES

[1] Manam NS, Harun WSW, Shri DNA, Ghani SAC, Kurniawan T, Ismail MH, et al. Study of corrosion in biocompatible metals for implants : A review. J Alloys Compd 2017;701:698–715. https://doi.org/10.1016/j.jallcom.2017.01.196.

[2] Garcia-Falcon CM, Gil-Lopez T, Verdu-Vazquez A, Mirza-Rosca JC. Electrochemical characterization of some cobalt base alloys in Ringer solution. Mater Chem Phys 2021;260:124164. https://doi.org/10.1016/j.matchemphys.2020.124164.

[3] Ramírez-Ledesma AL, Roncagliolo P, Álvarez-Pérez MA, Lopez HF, Juárez-Islas JA. Corrosion Assessment of an Implantable Dental Co-Cr Alloy in Artificial Saliva and Biocompatibility Behavior. J Mater Eng Perform 2020;29:1657–70. https://doi.org/10.1007/s11665-020-04711-2.

[4] Garcia-Falcon CM, Gil-Lopez T, Verdu-Vazquez A, Mirza-Rosca JC. Corrosion behavior in Ringer solution of several commercially used metal alloys. Anti-Corrosion Methods Mater 2021;68:324–30. https://doi.org/10.1108/ACMM-05-2021-2486.

[5] Alloys CD, Garcia-falcon CM, Gil-lopez T, Verdu-vazquez A, Mirza-rosca JC. Analysis and Comparison of the Corrosive Behavior of Nickel-Based and Cobalt-Based Dental Alloys 2021:1–12.

[6] Liu Y, Gilbert JL. The e ff ect of simulated in fl ammatory conditions and pH on fretting corrosion of CoCrMo alloy surfaces 2017;391:302–11. https://doi.org/10.1016/j.wear.2017.08.011.

[7] Perdomo-Socorro PP, Florido-Suárez NR, Verdú-Vázquez A, Mirza-Rosca JC. Comparative EIS study of titanium-based materials in high corrosive environments. Int J Surf Sci Eng 2021;15:152–64. https://doi.org/10.1504/IJSURFSE.2021.116333.

[8] The authors acknowledge the structural founds project CABINFR2019-07 for providing the infrastructure used in this work.